

Net influence of an internally-generated QBO

M. M. Hurwitz et al.

Net influence of an internally-generated QBO on modelled stratospheric climate and chemistry

M. M. Hurwitz^{1,2}, L. D. Oman², P. A. Newman², and I.-S. Song³

¹Goddard Earth Science Technology and Research (GESTAR), Morgan State University, Baltimore, MD, USA

²NASA Goddard Space Flight Center, Greenbelt, MD, USA

³Korea Institute of Atmospheric Prediction Systems (KIAPS), Seoul, South Korea

Received: 22 March 2013 – Accepted: 6 May 2013 – Published: 23 May 2013

Correspondence to: M. M. Hurwitz (margaret.m.hurwitz@nasa.gov)

Published by Copernicus Publications on behalf of the European Geosciences Union.

Title Page

Abstract

Introduction

Conclusions

References

Tables

Figures

⏪

⏩

◀

▶

Back

Close

Full Screen / Esc

Printer-friendly Version

Interactive Discussion



Abstract

A Goddard Earth Observing System Chemistry–Climate Model (GEOSCCM) simulation with strong tropical non-orographic gravity wave drag (GWD) is compared to an otherwise identical simulation with near-zero tropical non-orographic GWD. The GEOSCCM generates a quasi-biennial oscillation (QBO) zonal wind signal in response to strong, quasi-realistic tropical GWD. The modelled QBO has a frequency and amplitude that closely resembles observations. In the annual mean, the modelled QBO improves the simulation of tropical zonal winds and enhances tropical and sub-tropical stratospheric variability. Also, inclusion of the QBO slows the meridional overturning circulation, resulting in a generally older stratospheric mean age-of-air. Slowing of the overturning circulation, changes in stratospheric temperature and enhanced sub-tropical mixing all affect the mean distributions of ozone, methane and nitrous oxide. Furthermore, the modelled QBO enhances polar stratospheric variability in winter. Because tropical zonal winds are easterly in the simulation without a QBO, there is a relative increase in tropical zonal winds in the simulation with a QBO. Extra-tropical differences between the simulations with and without a QBO thus reflect a bias toward the westerly phase of the QBO: a relative strengthening of the polar stratospheric jet, polar stratospheric cooling and a weak reduction in Arctic lower stratospheric ozone.

1 Introduction

The quasi-biennial oscillation (QBO) is the leading mode of variability in the tropical lower and middle stratosphere (Baldwin et al., 2001). The QBO is characterized by a downward-propagating pattern of alternating easterly and westerly zonal winds in the equatorial region, with a period of approximately 28 months, and is driven by both gravity and planetary-scale waves (Reed et al., 1961). The zonal wind QBO induces changes in the tropical stratospheric circulation, affecting the concentrations of ozone and other trace constituents (Gray et al., 1989; Butchart et al., 2003; Tian et al., 2006).

Net influence of an internally-generated QBO

M. M. Hurwitz et al.

Title Page

Abstract

Introduction

Conclusions

References

Tables

Figures



Back

Close

Full Screen / Esc

Printer-friendly Version

Interactive Discussion



Hurwitz et al., 2011b) can internally-generate a QBO with a realistic periodicity and amplitude, depending on the latitudinal structure of the non-orographic gravity wave drag (GWD). Comparing two simulations using this formulation of the GEOSCCM, one with a QBO and another without, this paper quantifies the net effect of the modelled QBO on stratospheric climate and variability. Section 2 provides a brief description of the GEOSCCM, as well as the two above-mentioned simulations. The net effects of the modelled QBO on the mean and variance of stratospheric zonal winds, temperature, mean age, ozone and methane are shown in Sect. 3. Section 4 provides a summary and brief discussion.

2 Model and simulations

This paper considers the net impact of the QBO in Version 2 of the GEOSCCM. The GEOSCCM couples the GEOS-5 general circulation model (Molod et al., 2012) with a comprehensive stratospheric chemistry module (Pawson et al., 2008). The GEOSCCM performed well in the SPARC CCMVal (2010) detailed evaluation of stratospheric processes. The present formulation of the GEOSCCM is the same as in Hurwitz et al. (2011b). In this formulation, the model has 2° latitude \times 2.5° longitude horizontal resolution and 72 vertical layers, with a model top at 0.01 hPa. Predicted distributions of water vapour, ozone, primary greenhouse gases (CO_2 , CH_4 , and N_2O), CFC-11, CFC-12 and HCFC-22 feed back to the radiative calculations.

In the GEOSCCM, tropical stratospheric zonal wind variability depends on the details of the non-orographic GWD scheme. As non-orographic gravity waves often accompany precipitation (e.g., convective and frontal systems; see Richter et al., 2010), the latitudinal structure of the gravity wave spectrum is designed to mimic the structure of the climatological mean precipitation field (solid black line in Fig. 5 of Molod et al., 2012). A 700 km wavelength is used for the tropical non-orographic waves to prevent an excessive downward propagation of the semi-annual oscillation into the lower stratosphere, and thus contamination of the QBO signal. With a tropical peak in

Net influence of an internally-generated QBO

M. M. Hurwitz et al.

Title Page

Abstract

Introduction

Conclusions

References

Tables

Figures



Back

Close

Full Screen / Esc

Printer-friendly Version

Interactive Discussion



Net influence of an internally-generated QBO

M. M. Hurwitz et al.

Title Page

Abstract

Introduction

Conclusions

References

Tables

Figures



Back

Close

Full Screen / Esc

Printer-friendly Version

Interactive Discussion



non-orographic gravity wave stress, the present model formulation generates a QBO signal in equatorial zonal winds (see Sect. 3.1). Prior to this model formulation, the GEOSCCM did not generate a QBO i.e., zonal winds in the equatorial lower stratosphere were generally easterly (see Fig. 1c and SPARC CCMVal, 2010).

Two GEOSCCM simulations are used to assess the net stratospheric impacts of the QBO. The two simulations are identical, except for the magnitude of the non-orographic GWD stress applied in the deep tropics. The first simulation (hereafter “Q”) has a strong, quasi-realistic peak in tropical GWD, which as described above, generates a QBO signal. The second simulation (hereafter “N”) has weak tropical GWD stress (dashed black line in Fig. 5 of Molod et al., 2012), and thus does not have a QBO.

Both simulations are 50 yr “time-slice” simulations with fixed climate forcings and annually repeating sea surface temperature (SST) and sea ice climatologies. Surface mixing ratios of the primary greenhouse gases and ozone-depleting substances are specified from 2005 concentrations. The SST and sea ice climatologies are composites of 10 ENSO neutral years that span the satellite era (as in Hurwitz et al., 2011b). HadISST1 SSTs and sea ice concentrations at $1^\circ \times 1^\circ$ resolution (Rayner et al., 2003) are used to prepare the composites. Variability related to the solar cycle and volcanic eruptions is not considered.

Modelled temperature and zonal wind fields are compared with the Modern Era Retrospective-Analysis for Research and Applications (MERRA). MERRA is a meteorological reanalysis, based on an extensive set of satellite observations and on the Goddard Earth Observing System Data Analysis System, Version 5 (GEOS-5), from 1979 through the present (Rienecker et al., 2011). The MERRA reanalysis has vertical coverage up to 0.1 hPa, and for this study, is interpolated to $1.25^\circ \times 1.25^\circ$ horizontal resolution.

Additionally, simulated stratospheric mean age-of-air, ozone, nitrous oxide and methane are compared with observational datasets. Simulated mean age-of-air is compared with profiles derived from CO_2 and SF_6 observations (Andrews et al., 2001; En-

gel et al., 2009). These observations were taken between 1986 and 2005. Simulated ozone (O_3) and nitrous oxide (N_2O) are compared with the 2004–2012 climatology of the Aura Microwave Limb Sounder (MLS) version 3.3 O_3 and N_2O products (Froidevaux et al., 2008; Jiang et al., 2007; Livesey et al., 2008, 2011). Simulated methane (CH_4) is compared with the UARS HALOE climatology for 1991–2002 (Russell et al., 1993; Grooss et al., 2005). The UARS HALOE climatology is scaled by 1.02 to reflect the increase in methane surface mixing ratio between the mid-1990s and 2005 (see <http://www.esrl.noaa.gov>). More details about each dataset are provided in Chapter 1 of SPARC CCMVal (2010).

3 Results

3.1 Equatorial zonal winds

The QBO in zonal winds is well simulated in Q. The left-hand panels of Fig. 1 show 10 yr timeseries of equatorial winds in the MERRA reanalysis (1990–1999; Fig. 1a), Q (Fig. 1c) and N (Fig. 1e). The right-hand panels of Fig. 1 show the frequency spectra for equatorial winds for 1979–2012 in MERRA (Fig. 1b) and for the entire Q and N simulations (Fig. 1d, f). The simulated QBO signal has realistic amplitude and periodicity (compare Fig. 1a and c). In Q, the simulated peak frequency is 27 months at 30 hPa (Fig. 1d), with a secondary peak at 25 months, compared with 28 months in the MERRA reanalysis (Fig. 1b). In the upper and middle stratosphere, the annual (12 month) and semi-annual (6 month) frequencies are well simulated. Note that the simulated QBO signal is weaker than observed below 50 hPa (Hurwitz et al., 2011b).

Equatorial zonal winds are easterly throughout the N simulation, without a QBO signal (Fig. 1e). That is, lower stratospheric zonal wind variability is negligible. However, the annual and semi-annual frequencies are simulated in the middle and upper stratosphere (Fig. 1f).

Title Page

Abstract

Introduction

Conclusions

References

Tables

Figures



Back

Close

Full Screen / Esc

Printer-friendly Version

Interactive Discussion



3.2 Annual mean impact of the QBO

Inclusion of the QBO impacts stratospheric mean climate and variability. Figures 2–4 show the 50 yr annual mean zonal wind, temperature, age-of-air, residual vertical and meridional velocities, methane, nitrous oxide and ozone fields in the Q simulation (left-hand panels), differences between Q and N (i.e., the net mean impact of the QBO) (middle panels), and QBO-related changes in stratospheric variability (right-hand panels). Annual and zonal mean zonal winds in the Q simulation are easterly in the tropical stratosphere and westerly in the extra-tropics (Fig. 2a), in good agreement with observations (black contours). In N, tropical stratospheric easterlies are on average stronger than in the MERRA reanalysis (not shown); thus, inclusion of the QBO represents both a relative zonal wind increase in the tropics ($10\text{--}20\text{ m s}^{-1}$) and an improvement in the simulated mean comparison with MERRA (Fig. 2b). As expected, zonal wind variability increases by 3–5 times in Q, as compared with N, throughout the tropical stratosphere (Fig. 2c).

The modelled stratospheric temperatures generally agree well with MERRA (Fig. 2d). A modest cold bias around 60° S may reflect the overly strong polar jet and delayed breakup of the Antarctic vortex in austral spring (Hurwitz et al., 2010). Inclusion of the QBO contributes to this bias: the QBO warms the tropical stratosphere and Arctic lower stratosphere by $\sim 1\text{ K}$, but cools the Antarctic stratosphere by $\sim 1\text{ K}$ (Fig. 2e). QBO-related increases in temperature variability maximize in the middle stratosphere, in the deep tropics, with an additional lobe of increased variability around 30° S (Fig. 2f).

Inclusion of the QBO acts to slow the stratospheric circulation. Age-of-air is an indicator of the strength and structure of the meridional overturning (i.e., Brewer–Dobson) circulation (SPARC CCMVal, 2010). In the GEOSCCM, mean age is an inert tracer that measures the time since a parcel of air has left the troposphere. Because most air enters the stratosphere in the tropics, mean age values are lowest in the tropical lower stratosphere and highest in the high latitude upper and middle stratosphere (Fig. 3a). Q–N differences in annual mean age are generally positive throughout the stratosphere

ACPD

13, 13495–13518, 2013

Net influence of an internally-generated QBO

M. M. Hurwitz et al.

Title Page

Abstract

Introduction

Conclusions

References

Tables

Figures

◀

▶

◀

▶

Back

Close

Full Screen / Esc

Printer-friendly Version

Interactive Discussion



i.e., the QBO slows the overturning circulation (Fig. 3b). The largest increases in mean age (~ 0.3 yr) are seen in the tropical stratosphere around 10 hPa. Figure 5 shows observed and simulated mean age-of-air profiles in the deep tropics. While the mean age in N falls within the observational error, the older tropical mean age in the Q simulation is in better agreement with CO_2 and SF_6 observations. QBO-related changes in mean age variability, similarly to temperature variability, peak in the Southern Hemisphere tropical middle stratosphere (Fig. 3c). Decreased mean age in the lower stratosphere is consistent with slowing of the overturning circulation: less older air is advected downward into the mid-latitudes.

QBO-related changes in the residual circulation are consistent with the changes in mean age-of-air. In the upper stratosphere and polar regions, the net impact of the QBO is dominated by the slowing of the meridional circulation. At and above 10 hPa, Q–N differences in w^* (residual vertical velocity) oppose the w^* climatology: negative differences in the tropics (weakened upwelling), and positive differences in the extra-tropics (weakened downwelling; compare Fig. 3d and e). Weakened tropical upwelling enhances tropical water vapour concentrations in the tropical stratosphere (not shown). In Fig. 3g–i, positive v^* (residual meridional velocity) values indicate poleward motion in both hemispheres. Negative differences in v^* , e.g. around 3 hPa in the tropics and in the uppermost polar stratosphere reflect weakened poleward transport (Fig. 3b). In the lower and middle stratosphere, the net impact of the QBO is to enhance poleward transport. That is, positive v^* between 10 and 70 hPa, in the tropics and mid-latitudes, is consistent with enhanced mixing in this region. Note that the v^* differences are largest in the Southern Hemisphere and coincident with the peak change in v^* variability (Fig. 3i). Below 70 hPa, tropical v^* is positive. This set of v^* changes is consistent with the narrowing but strengthening of upward transport in the tropical lower stratosphere (Fig. 3e).

Both slowing of the stratospheric overturning circulation and enhanced lower stratospheric mixing affect the distribution of methane. Since methane is mainly transported into the stratosphere in the deep tropics, the distribution of stratospheric methane is

Net influence of an internally-generated QBO

M. M. Hurwitz et al.

Title Page

Abstract

Introduction

Conclusions

References

Tables

Figures

◀

▶

◀

▶

Back

Close

Full Screen / Esc

Printer-friendly Version

Interactive Discussion



Net influence of an internally-generated QBO

M. M. Hurwitz et al.

Title Page

Abstract

Introduction

Conclusions

References

Tables

Figures

◀

▶

◀

▶

Back

Close

Full Screen / Esc

Printer-friendly Version

Interactive Discussion



inverted as compared with mean age: the highest concentrations are found in the tropical lower stratosphere, while the lowest values are found in the polar upper stratosphere. The structure of the simulated tropical and subtropical methane distribution matches the scaled UARS HALOE climatology, but with a high bias (Fig. 4a). This bias results from the stronger than observed transport in the GEOSCCM (SPARC CCMVal, 2010). Inclusion of the QBO decreases tropical and upper stratospheric methane mixing ratios, reflecting slowing of the stratospheric circulation (Fig. 4b). Given the negative latitudinal gradient in methane concentrations (Fig. 4a), increased lower stratospheric methane suggests enhanced meridional mixing, i.e. weakening of the subtropical transport barrier (Fig. 4b); this effect is further discussed below. Inclusion of the QBO generally increases methane variability, with the largest increases in the tropics and sub-tropical Southern Hemisphere (Fig. 4c).

QBO-related changes in N_2O provide further evidence for enhanced sub-tropical mixing. Similarly to methane, the highest N_2O concentrations are found in the tropical lower stratosphere, while the lowest values are found in the upper stratosphere (Fig. 4d). The simulated N_2O distribution matches the MLS climatology, but with a high bias in the tropical lower stratosphere, similar to the methane bias. Inclusion of the QBO weakens the meridional gradient of N_2O : decreasing equatorial N_2O (exceeding 30 ppbv) and increasing N_2O at sub-tropical latitudes (up to 10 ppbv) (Fig. 4e). Figure 6 shows the annual cycle of Q–N differences in the sub-tropical N_2O gradient. Mean N_2O differences between 10 and 40°s latitude serve as a proxy for the strength of the sub-tropical gradient i.e., the strength of the sub-tropical mixing barrier. Negative differences indicate a weakening of the sub-tropical N_2O gradient, due to enhanced mixing (Douglass et al., 1999). The largest changes in sub-tropical N_2O are centred around 10 hPa (consistent with the increases in sub-tropical v^* and methane), in winter months. The QBO has a larger impact on sub-tropical N_2O in the SH (Fig. 6a) than in the NH (Fig. 6b), consistent with the relatively larger enhancements in variability in the SH (Figs. 2–4, right-hand panels).

Net influence of an internally-generated QBO

M. M. Hurwitz et al.

Title Page

Abstract

Introduction

Conclusions

References

Tables

Figures

◀

▶

◀

▶

Back

Close

Full Screen / Esc

Printer-friendly Version

Interactive Discussion



The net impact of the QBO on ozone reflects warming of the tropical stratosphere, enhanced sub-tropical mixing and slowing of the stratospheric overturning circulation. The annual mean ozone mixing ratio maximizes at approximately 10 ppmv in the deep tropics, at 10 hPa, and decreases with latitude (Fig. 4g). Simulated ozone is generally in agreement with the MLS ozone climatology. Thus, inclusion of the QBO improves model performance; the peak in ozone mixing ratio around 10 hPa is ~ 0.8 ppmv too high in the N simulation. Relative warming of the tropical middle stratosphere in Q contributes to the negative ozone differences in the deep tropics (Figs. 2e and 4h). However, at the equator at 10 hPa, the ratio between temperature and ozone differences (i.e., $\Delta T/\Delta O_3 = 0.72 \text{ K}/0.8 \text{ ppmv} = 0.9$) does not agree with the ratio of ~ 6.7 as determined by Oman et al. (2010). This result suggests that other mechanisms contribute to the change in tropical ozone. Decreased tropical ozone at 10 hPa is consistent with both (1) strengthening of vertical upwelling below 10 hPa (Fig. 3e) and (2) enhanced mixing with mid-latitude air with relatively lower ozone concentrations (Figs. 4g and 6).

3.3 High latitude impact of the QBO in winter

In certain months, in the Q simulation, equatorial zonal winds at 30 hPa are positively correlated with zonal winds in the polar stratosphere (not shown). That is, the GEOSCCM reproduces the Holton–Tan (1980) relation between the phase of the QBO and polar vortex strength: the polar vortices are relatively stronger during the westerly phase of the QBO. In the GEOSCCM, equatorial zonal wind correlations with zonal winds at 60° S are strong in e.g., September (Fig. 7), and at 60° N in January (Fig. 8).

The net impact of the QBO on zonal winds and temperature (i.e., Q–N) mimics the differences between the westerly and easterly phases of the QBO (i.e., in the Q simulation), at Southern Hemisphere high latitudes in September. Inclusion of the QBO strengthens the Antarctic jet (around 60° S) by $5\text{--}10 \text{ m s}^{-1}$ (Fig. 7a). An equal strengthening is seen in Fig. 7b, which shows the zonal wind differences between the five Septembers in Q with the highest (i.e., QBO-W) equatorial zonal wind values at 30 hPa and the five Septembers in Q with the lowest (i.e., QBO-E) equatorial zonal wind val-

ues at 30 hPa. Note that the QBO-W–QBO-E differences are generally not statistically significant in the extra-tropics, due to the small size of the QBO-W and QBO-E composites.

Extra-tropical stratospheric temperatures decrease in September, consistent with the stronger zonal winds (i.e., by the thermal wind relation). Temperature differences are negative poleward of 45° S, both for Q–N and QBO-W–QBO-E, with peak differences of 5 K in the Antarctic (Fig. 7c, d). Tropical and mid-latitude Q–N differences reflect changes in stratospheric circulation and mixing (see Sect. 3.2).

Equivalent zonal wind and temperature differences are seen in the Northern Hemisphere extra-tropics in January. Q–N differences reflect a relative shift toward the westerly phase of the QBO: a relative strengthening of the Arctic stratospheric jet (Fig. 8a, b) and cooling throughout the extra-tropical stratosphere (Fig. 8c, d). In this case, zonal wind and temperature differences are larger in response to QBO phase as compared with the net impact of the QBO. Negative ozone differences in the Arctic lower stratosphere (Fig. 8e, f), though weak, hint at enhanced chemical ozone depletion, due to the cooler and more isolated polar air mass in January. The small size of the QBO-W and QBO-E composites likely weakens the statistical significance of the ozone differences.

4 Discussion

A model's representation of the QBO makes a significant difference to the mean stratospheric climate and variability. As expected, the addition of a QBO significantly enhances tropical variability. Extra-tropical zonal wind and temperature variability in winter is also enhanced. While the QBO is by definition an oscillating phenomenon, the multi-decadal mean of the modelled QBO modifies the average climate. In particular:

1. Adding an internal QBO signal affects the mean stratospheric climate.

In the GEOSCCM, inclusion of a QBO signal slows the meridional overturning circulation, leading to older mean age-of-air throughout the stratosphere and af-

Net influence of an internally-generated QBO

M. M. Hurwitz et al.

Title Page

Abstract

Introduction

Conclusions

References

Tables

Figures



Back

Close

Full Screen / Esc

Printer-friendly Version

Interactive Discussion



Net influence of an internally-generated QBO

M. M. Hurwitz et al.

Title Page

Abstract

Introduction

Conclusions

References

Tables

Figures

◀

▶

◀

▶

Back

Close

Full Screen / Esc

Printer-friendly Version

Interactive Discussion



fecting the distribution of trace species such as ozone, methane and nitrous oxide. The sub-tropical mixing barrier is weakened, enhancing methane and nitrous oxide in the extra-tropical lower stratosphere, and contributing the reduced peak ozone mixing ratio at 10 hPa. The polar vortices are strengthened, particularly in winter. The net dynamical and transport impacts of the QBO generally improve model performance.

2. The net impact of the QBO depends on both the baseline zonal wind field and the relative change in tropical zonal winds.

In the GEOSCCM, the baseline tropical zonal winds are easterly. In the simulation with a QBO signal, there is a relative increase in zonal winds in the tropical lower and middle stratosphere. Extra-tropical differences between the simulations with and without a QBO thus reflect a bias toward the westerly phase of the QBO: a relative cooling and strengthening of the polar vortices, and a weak reduction in Arctic lower stratospheric ozone. The annual mean impact of the QBO on the polar stratosphere is larger in the GEOSCCM (up to 12 ms^{-1} , in both hemispheres) than in the MAECHAM4-CHEM CCM (no significant zonal wind differences) (Punge and Giorgetta, 2008), likely reflecting larger tropical zonal wind differences between the QBO and “no QBO” GEOSCCM simulations and/or increased statistical robustness due to the greater length of the GEOSCCM simulations.

The QBO has a robust, net impact on the mean stratospheric climate and trace gas distributions. In the case of the GEOSCCM, inclusion of the QBO yields better agreement between the simulated fields and climatological averages derived from a meteorological reanalysis and satellite datasets of ozone, methane and nitrous oxide. While it is difficult to internally generate a QBO signal in a global climate model, a model with the ability to simulate a QBO presents significant advantages in predicting the future evolution of the stratosphere: climate change is likely to modify the GWD which will remotely modify stratospheric climate and variability.

Capturing this feedback will require a modelled QBO forced by an interactive GWD source spectrum, driven by changes in e.g., convective precipitation.

Acknowledgements. The authors thank NASA's MAP program for funding, S. M. Frith for processing the model output and S. Strahan for helpful discussions.

References

- Andrews, A. E., Boering, K. A., Daube, B. C., Wofsy, S. C., Loewenstein, M., Jost, H., Podolske, J. R., Webster, C. R., Herman, R. L., Scott, D. C., Flesch, G. J., Moyer, E. J., Elkins, J. W., Dutton, G. S., Hurst, D. F., Moore, F. L., Ray, E. A., Romashkin, P. A., and Strahan, S. E.: Mean ages of stratospheric air derived from in situ observations of CO₂, CH₄, and N₂O, *J. Geophys. Res.*, 106, 32295–32314, 2001.
- Baldwin, M. P. and Dunkerton, T. J.: Quasi-biennial modulation of the Southern Hemisphere stratospheric polar vortex, *Geophys. Res. Lett.*, 25, 3343–3346, 1998.
- Baldwin, M. P., Gray, L. J., Dunkerton, T. J., Hamilton, K., Haynes, P. H., Randel, W. J., Holton, J. R., Alexander, M. J., Hirota, I., Horinouchi, T., Jones, D. B. A., Kinnerson, J. S., Marquardt, C., Sato, K., and Takahashi, M.: The quasi-biennial oscillation, *Rev. Geophys.*, 39, 179–229, 2001.
- Butchart, N., Scaife, A. A., Austin, J., Hare, S. H. E., and Knight, J. R.: Quasi-biennial oscillation in ozone in a coupled chemistry-climate model, *J. Geophys. Res.*, 108, D15, doi:10.1029/2002JD003004, 2003.
- Douglass, A. R., Prather, M. J., Hall, T. M., Strahan, S. E., Rasch, P. J., Sparling, L. C., Coy, L., and Rodriguez, J. M.: Choosing meteorological input for the global modelling initiative assessment of high-speed aircraft, *J. Geophys. Res.*, 104, 27545–27564, 1999.
- Engel, A., Mobius, T., Bonisch, H., Schmidt, U., Heinz, R., Levin, I., Atlas, E., Aoki, S., Nakazawa, T., Sugawara, S., Moore, F., Hurst, D., Elkins, J., Schauffler, S., Andrews, A., and Boering, K.: Age of stratospheric air unchanged within uncertainties over the past 30 years, *Nat. Geosci.*, 2, 28–31, 2009.
- Froidevaux, L., Jiang, Y. B., Lambert, A., Livesey, N. J., Read, W. G., Waters, J. W., Browell, E. V., Hair, J. W., Avery, M. A., Mcgee, T. J., Twigg, L. W., Sumnicht, G. K., Jucks, K. W., Margitan, J. J., Sen, B., Stachnik, R. A., Toon, G. C., Bernath, P. F., Boone, C. D., Walker, K. A., Filipiak, M. J., Harwood, R. S., Fuller, R. A., Manney, G. L., Schwartz, M. J., Daffer,

Net influence of an internally-generated QBO

M. M. Hurwitz et al.

Title Page

Abstract

Introduction

Conclusions

References

Tables

Figures

◀

▶

◀

▶

Back

Close

Full Screen / Esc

Printer-friendly Version

Interactive Discussion



Net influence of an internally-generated QBO

M. M. Hurwitz et al.

Title Page

Abstract

Introduction

Conclusions

References

Tables

Figures

◀

▶

◀

▶

Back

Close

Full Screen / Esc

Printer-friendly Version

Interactive Discussion



W. H., Drouin, B. J., Cofield, R. E., Cuddy, D. T., Jarnot, R. F., Knosp, B. W., Perun, V. S., Snyder, W. V., Stek, P. C., Thurstans, R. P., and Wagner, P. A.: Validation of Aura Microwave Limb Sounder stratospheric and mesospheric ozone measurements, *J. Geophys. Res.*, 113, D15S20, doi:10.1029/2007JD008771, 2008.

5 Garfinkel, C. I. and Hartmann, D. L.: Effects of the El Niño-Southern Oscillation and the Quasi-Biennial Oscillation on polar temperatures in the stratosphere, *J. Geophys. Res.*, 112, D19112, doi:10.1029/2007JD008481, 2007.

Gray, L. J. and Pyle, J. A.: A two-dimensional model of the quasi-biennial oscillation of ozone, *J. Atmos. Sci.*, 46, 203–220, 1989.

10 Grooß, J.-U. and Russell III, J. M.: Technical note: A stratospheric climatology for O₃, H₂O, CH₄, NO_x, HCl and HF derived from HALOE measurements, *Atmos. Chem. Phys.*, 5, 2797–2807, doi:10.5194/acp-5-2797-2005, 2005.

Holton, J. R. and Tan, H.-C.: The Influence of the equatorial quasi-biennial oscillation on the global circulation at 50 mb, *J. Geophys. Res.*, 37, 2200–2208, 1980.

15 Hurwitz, M. M., Newman, P. A., Li, F., Oman, L. D., Morgenstern, O., Braesicke, P., and Pyle, J. A.: Assessment of the breakup of the Antarctic polar vortex in two new chemistry-climate models, *J. Geophys. Res.*, 115, D07105, doi:10.1029/2009JD012788, 2010.

Hurwitz, M. M., Newman, P. A., Oman, L. D., and Molod, A. M.: Response of the Antarctic stratosphere to two types of El Niño events, *J. Atmos. Sci.*, 68, 812–822, 2011a.

20 Hurwitz, M. M., Song, I.-S., Oman, L. D., Newman, P. A., Molod, A. M., Frith, S. M., and Nielsen, J. E.: Response of the Antarctic stratosphere to warm pool El Niño Events in the GEOS CCM, *Atmos. Chem. Phys.*, 11, 9659–9669, doi:10.5194/acp-11-9659-2011, 2011b.

Jiang, Y. B., Froidevaux, L., Lambert, A., Livesey, N. J., Read, W. G., Waters, J. W., Bojkov, B., Leblanc, T., McDermid, I. S., Godin-Beekmann, S., Filipiak, M. J., Harwood, R. S., Fuller, R. A., Daffer, W. H., Drouin, B. J., Cofield, R. E., Cuddy, D. T., Jarnot, R. F., Knosp, B. W., Perun, V. S., Schwartz, M. J., Snyder, W. V., Stek, P. C., Thurstans, R. P., Wagner, P. A., Allaart, M., Andersen, S. B., Bodeker, G., Calpini, B., Claude, H., Coetzee, G., Davies, J., De Backer, H., Dier, H., Fujiwara, M., Johnson, B., Kelder, H., Leme, N. P., Konig-Langlo, G., Kyro, E., Laneve, G., Fook, L. S., Merrill, J., Morris, G., Newchurch, M., Oltmans, S., Parrondos, M. C., Posny, F., Schmidlin, F., Skrivankova, P., Stubi, R., Tarasick, D., Thompson, A., Thouret, V., Viatte, P., Vomel, H., von Der Gathen, P., Yela, M., and Zabolocki, G.: Validation of the Aura Microwave Limb Sounder ozone by ozonesonde and lidar measurements, *J. Geophys. Res.*, 112, D24S34, doi:10.1029/2007JD008776, 2007.

Net influence of an internally-generated QBO

M. M. Hurwitz et al.

Title Page

Abstract

Introduction

Conclusions

References

Tables

Figures

◀

▶

◀

▶

Back

Close

Full Screen / Esc

Printer-friendly Version

Interactive Discussion



- Lait, L. R., Schoeberl, M. R., and Newman, P. A.: Quasi-biennial modulation of the Antarctic ozone depletion, *J. Geophys. Res.*, 94, 11559–11571, 1989.
- Livesey, N. J., Filipiak, M. J., Froidevaux, L., Read, W. G., Lambert, A., Santee, M. L., Jiang, J. H., Pumphrey, H. C., Waters, J. W., Cofield, R. E., Cuddy, D. T., Daffer, W. H., Drouin, B. J., Fuller, R. A., Jarnot, R. F., Jiang, Y. B., Knosp, B. W., Li, Q. B., Perun, V. S., Schwartz, M. J., Snyder, W. V., Stek, P. C., Thurstans, R. P., Wagner, P. A., Avery, M., Browell, E. V., Cammas, J. P., Christensen, L. E., Diskin, G. S., Gao, R.-S., Jost, H. J., Loewenstein, M., Lopez, J. D., Nedelec, P., Osterman, G. B., Sachse, G. W., and Webster, C. R.: Validation of Aura Microwave Limb Sounder O₃ and CO observations in the upper troposphere and lower stratosphere, *J. Geophys. Res.*, 113, D15S02, doi:10.1029/2007JD008805, 2008.
- Livesey, N. J., Read, W. G., Froidevaux, L., Lambert, A., Manney, G. L., Pumphrey, H. C., Santee, M. L., Schwartz, M. J., Wang, S., Cofeld, R. E., Cuddy, D. T., Fuller, R. A., Jarnot, R. F., Jiang, J. H., Knosp, B. W., Stek, P. C., Wagner, P. A., and Wu, D. L.: Earth Observing System (EOS) Aura Microwave Limb Sounder (MLS) Version 3.3 Level 2 data quality and description document, JPL D-33509, 2011.
- Lu, H., Baldwin, M. P., Gray, L. J., and Jarvis, M. J.: Decadal-scale changes in the effect of the QBO on the northern stratospheric polar vortex, *J. Geophys. Res.*, 113, D10114, doi:10.1029/2007JD009647, 2008.
- Molod, A., Takacs, L., Suarez, M., Bacmeister, J., Song, I.-S., and Eichmann, A.: The GEOS-5 Atmospheric General Circulation Model: Mean climate and development from MERRA to Fortuna, Technical Report Series on Global Modeling and Data Assimilation, Vol. 28., available at: <http://gmao.gsfc.nasa.gov/pubs/docs/Molod484.pdf>, 2012.
- Oman, L. D., Waugh, D. W., Kawa, S. R., Stolarski, R. S., Douglass, A. R., and Newman, P. A.: Mechanisms and feedback causing changes in upper stratospheric ozone in the 21st century, *J. Geophys. Res.*, 115, D05303, doi:10.1029/2009JD012397, 2010.
- Pawson, S., Stolarski, R. S., Douglass, A. R., Newman, P. A., Nielsen, J. E., Frith, S. M., and Gupta, M. L.: Goddard Earth Observing System chemistry–climate model simulations of stratospheric ozone-temperature coupling between 1950 and 2005, *J. Geophys. Res.*, 113, D12103, doi:10.1029/2007JD009511, 2008.
- Punge, H. J. and Giorgetta, M. A.: Net effect of the QBO in a chemistry climate model, *Atmos. Chem. Phys.*, 8, 6505–6525, doi:10.5194/acp-8-6505-2008, 2008.
- Randel, W. J. and Cobb, J. B.: Coherent variations of monthly mean total ozone and lower stratospheric temperature, *J. Geophys. Res.*, 99, 5433–5447, 1994.

Net influence of an internally-generated QBO

M. M. Hurwitz et al.

Title Page

Abstract

Introduction

Conclusions

References

Tables

Figures

◀

▶

◀

▶

Back

Close

Full Screen / Esc

Printer-friendly Version

Interactive Discussion



- Rayner, N. A., Parker, D. E., Horton, E. B., Folland, C. K., Alexander, L. V., Rowell, D. P., and Kaplan, A.: Global analyses of sea surface temperature, sea ice, and night marine air temperature since the late nineteenth century, *J. Geophys. Res.*, 108, D14, 4407, doi:10.1029/2002JD002670, 2003.
- 5 Reed, R. J., Rasmusse, L. A., Campbell, W. J., and Rogers, D. G.: Evidence of a downward-propagating, annual wind reversal in equatorial stratosphere, *J. Geophys. Res.*, 66, 813–816, doi:10.1029/JZ066i003p00813, 1961.
- Richter, J. H., Sassi, F., and Garcia, R. R.: Toward a physically based gravity wave source parameterization in a general circulation model, *J. Atmos. Sci.*, 67, 136–156, 2010.
- 10 Rienecker, M. M., Suarez, M. J., Gelaro, R., Todling, R., Bacmeister, J., Liu, E., Bosilovich, M. G., Schubert, S. D., Takacs, L., Kim, G. K., Bloom, S., Chen, J. Y., Collins, D., Conaty, A., Da Silva, A., Gu, W., Joiner, J., Koster, R. D., Lucchesi, R., Molod, A., Owens, T., Pawson, S., Pegion, P., Redder, C. R., Reichle, R., Robertson, F. R., Ruddick, A. G., Sienkiewicz, M., and Woollen, J.: MERRA – NASA’s modern-era retrospective analysis for research and applications, *J. Climate*, 24, 3624–3648, doi:10.1175/JCLI-D-11-00015.1, 2011.
- 15 Russell, J. M., Gordley, L. L., Park, J. H., Drayson, S. R., Tuck, A. F., Harries, J. E., Cicerone, R. J., Crutzen, P. J., and Frederick, J. E.: The halogen occultation experiment, *J. Geophys. Res.*, 98, 10777–10797, 1993.
- SPARC CCMVal: SPARC report on the evaluation of chemistry–climate models, edited by: Eyring, V., Shepherd, T. G., and Waugh, D. W., SPARC Report No. 5, WCRP-132, WMO/TDNo. 1526, available at: <http://www.atmosp.physics.utoronto.ca/SPARC>, 2010.
- 20 Tian, W. S., Chipperfield, M. P., Gray, L. J., and Zawodny, J. M.: Quasi-biennial oscillation and tracer distributions in a coupled chemistry–climate model, *J. Geophys. Res.*, 111, D20301, doi:10.1029/2005JD006871, 2006.

Net influence of an internally-generated QBO

M. M. Hurwitz et al.

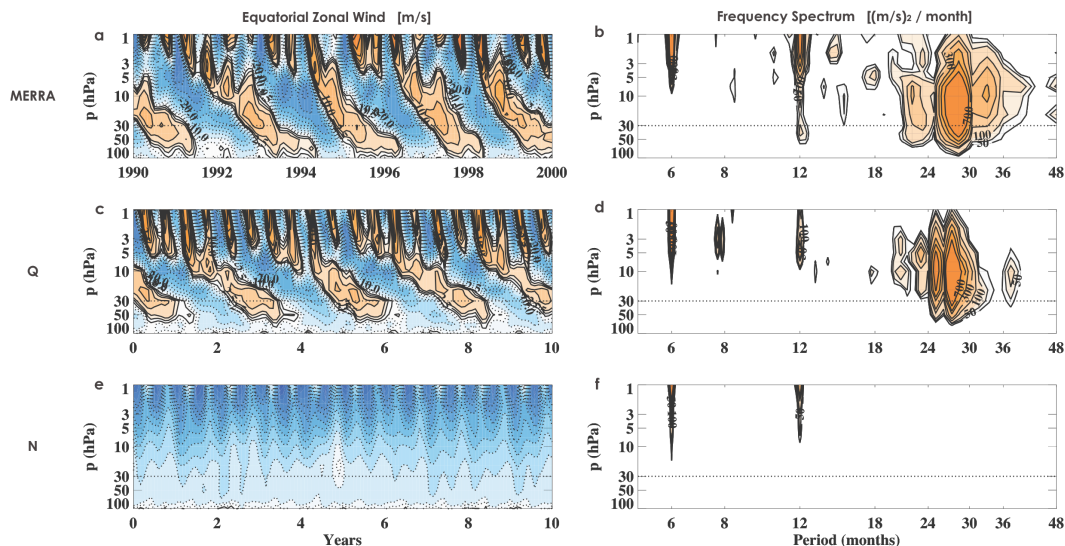


Fig. 1. Equatorial (4°S – 4°N) zonal wind [m s^{-1}] in (a, b) MERRA reanalysis, 1979–2009, (c, d) the Q simulation, and (e, f) the N simulation. (a, c, e) 10 yr timeseries. (b, d, f) frequency spectra for the entire span of the MERRA reanalysis and GEOSCCM simulation. Black dotted lines indicate the 30 hPa level.

[Title Page](#)
[Abstract](#)
[Introduction](#)
[Conclusions](#)
[References](#)
[Tables](#)
[Figures](#)
[◀](#)
[▶](#)
[◀](#)
[▶](#)
[Back](#)
[Close](#)
[Full Screen / Esc](#)
[Printer-friendly Version](#)
[Interactive Discussion](#)

Net influence of an internally-generated QBO

M. M. Hurwitz et al.

Title Page

Abstract

Introduction

Conclusions

References

Tables

Figures

◀

▶

◀

▶

Back

Close

Full Screen / Esc

Printer-friendly Version

Interactive Discussion

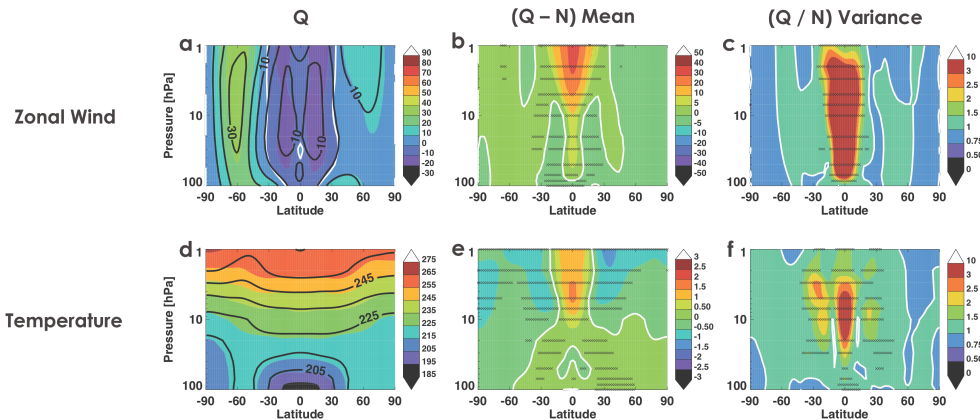


Fig. 2. (a–c) Zonal wind [m s^{-1}] and (d–f) temperature [K], for (a, d) Q zonal and annual mean; black contours indicate MERRA reanalysis mean for 2000–2010. (b, e) Q–N mean differences; white contours indicate zero difference. (c, f) Q/N changes in variance; white contours indicate where the ratio is equal to one. Black Xs indicate changes significant at the 95% level in a two-tailed t test.

Net influence of an internally-generated QBO

M. M. Hurwitz et al.

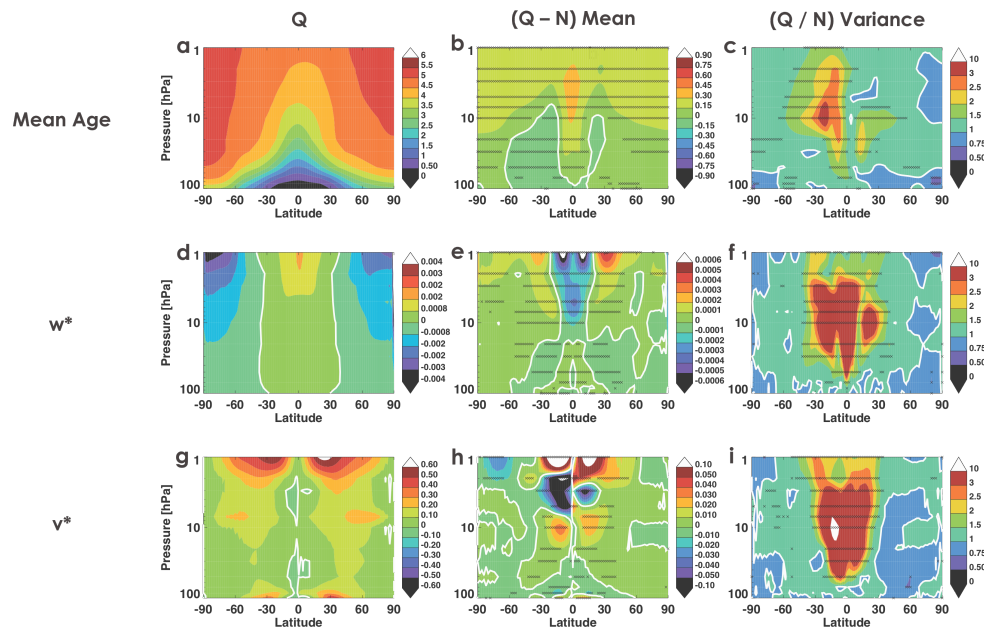


Fig. 3. As for Fig. 2, but for **(a–c)** mean age [years], **(d–f)** w^* [ms^{-1}] and **(g–i)** v^* [ms^{-1}].

Title Page

Abstract

Introduction

Conclusions

References

Tables

Figures

◀

▶

◀

▶

Back

Close

Full Screen / Esc

Printer-friendly Version

Interactive Discussion



Net influence of an internally-generated QBO

M. M. Hurwitz et al.

Title Page

Abstract

Introduction

Conclusions

References

Tables

Figures

◀

▶

◀

▶

Back

Close

Full Screen / Esc

Printer-friendly Version

Interactive Discussion

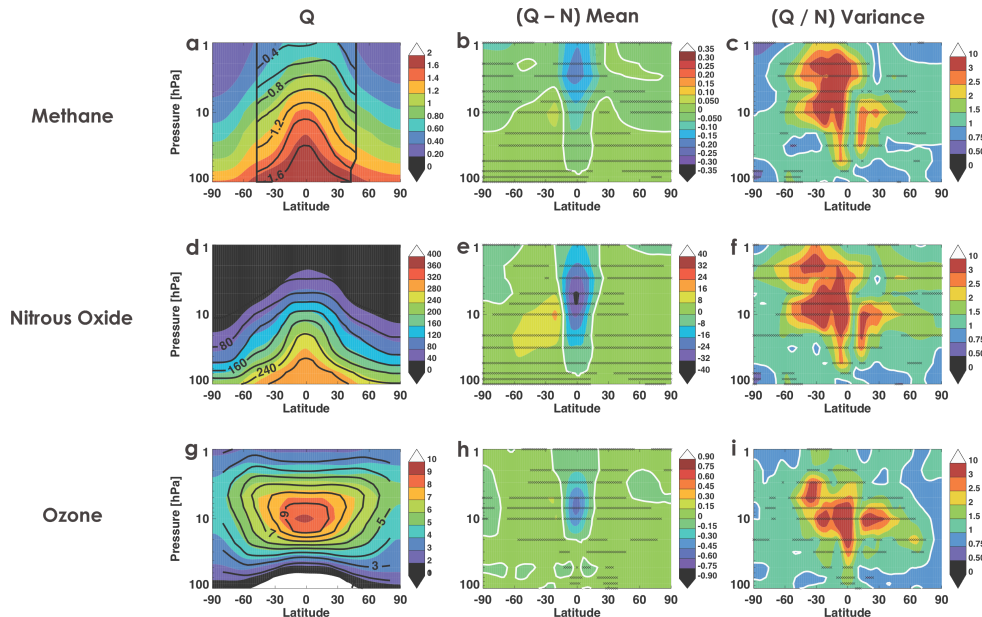


Fig. 4. As for Fig. 2, but for (a–c) methane [ppmv], (d–f) nitrous oxide [ppbv] and (g–i) ozone [ppmv]. Black contours in (a) indicate the scaled HALOE climatology; black contours in (d, g) indicate the MLS climatology.

Net influence of an internally-generated QBO

M. M. Hurwitz et al.

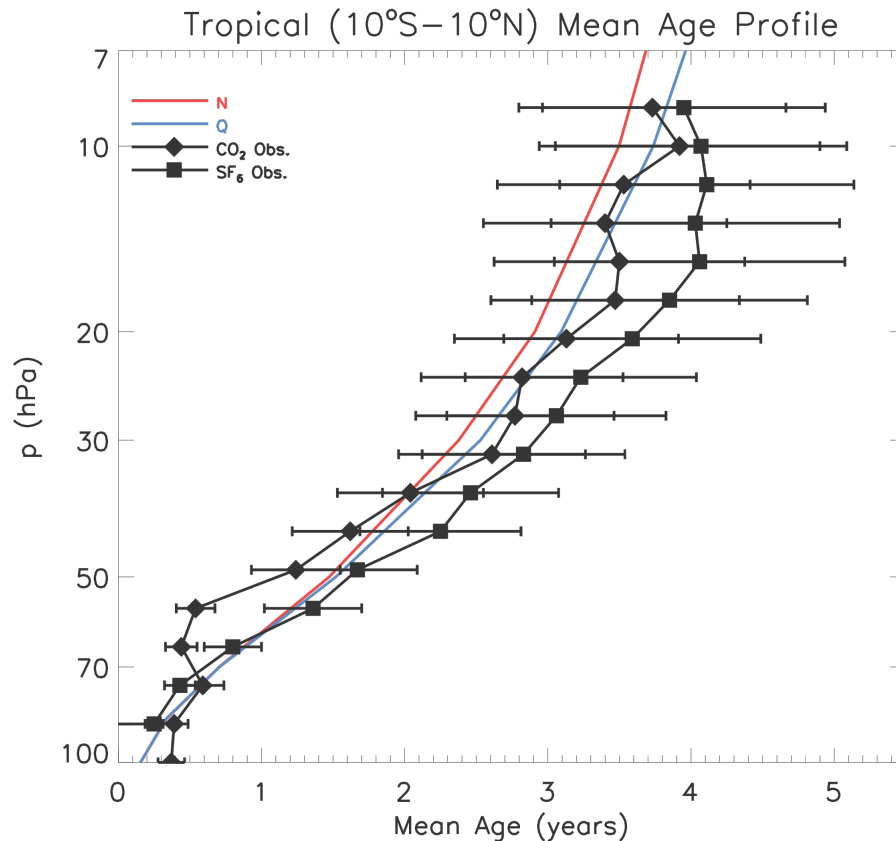


Fig. 5. Equatorial (10°S–10°N) mean age [yr] profiles in the N simulation (red), Q simulation (blue), and from CO₂ (black diamonds) and SF₆ (black squares) observations.

Title Page

Abstract Introduction

Conclusions References

Tables Figures

◀ ▶

◀ ▶

Back Close

Full Screen / Esc

Printer-friendly Version

Interactive Discussion



Net influence of an internally-generated QBO

M. M. Hurwitz et al.

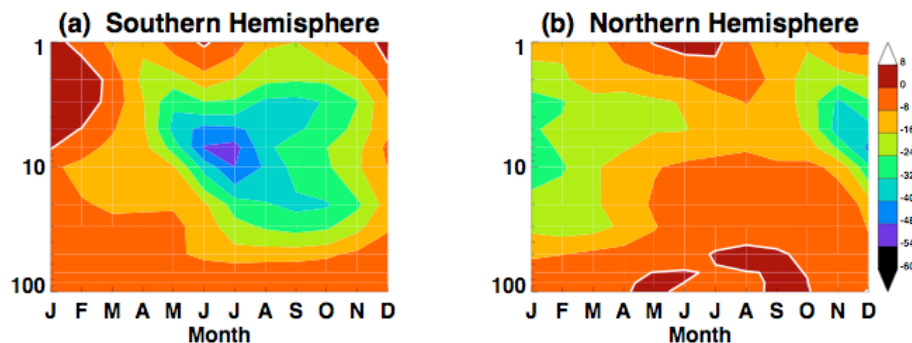


Fig. 6. Q–N differences in the subtropical N_2O gradient [ppbv], as a function of month and altitude in **(a)** the Southern Hemisphere and **(b)** the Northern Hemisphere. Negative differences indicate weakening of the sub-tropical mixing barrier i.e., enhanced sub-tropical mixing.

[Title Page](#)[Abstract](#)[Introduction](#)[Conclusions](#)[References](#)[Tables](#)[Figures](#)[◀](#)[▶](#)[◀](#)[▶](#)[Back](#)[Close](#)[Full Screen / Esc](#)[Printer-friendly Version](#)[Interactive Discussion](#)

Net influence of an internally-generated QBO

M. M. Hurwitz et al.

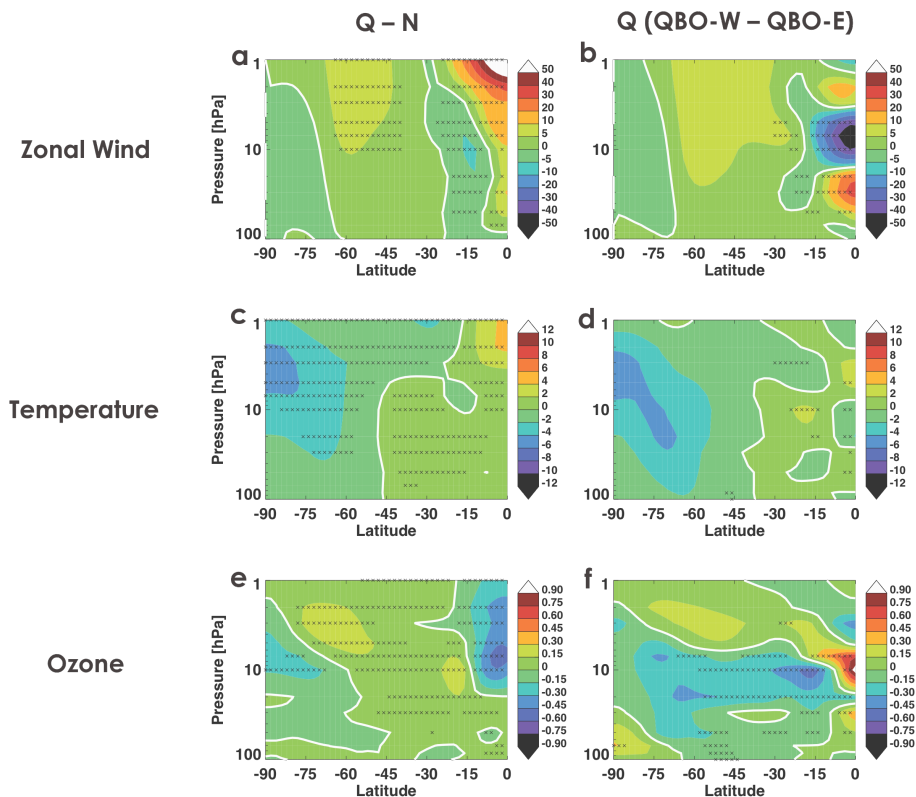


Fig. 7. September (a, b) zonal wind [ms^{-1}], (c, d) temperature [K] and (e, f) ozone [ppmv] differences in the Southern Hemisphere. (a, c, e) Q–N mean differences; (b, d, f) QBO-westerly – QBO-easterly differences in the Q simulation. White contours indicate zero difference. Black Xs indicate differences significant at the 95 % level in a two-tailed t test.

[Title Page](#)
[Abstract](#)
[Introduction](#)
[Conclusions](#)
[References](#)
[Tables](#)
[Figures](#)
[Back](#)
[Close](#)
[Full Screen / Esc](#)
[Printer-friendly Version](#)
[Interactive Discussion](#)

Net influence of an internally-generated QBO

M. M. Hurwitz et al.

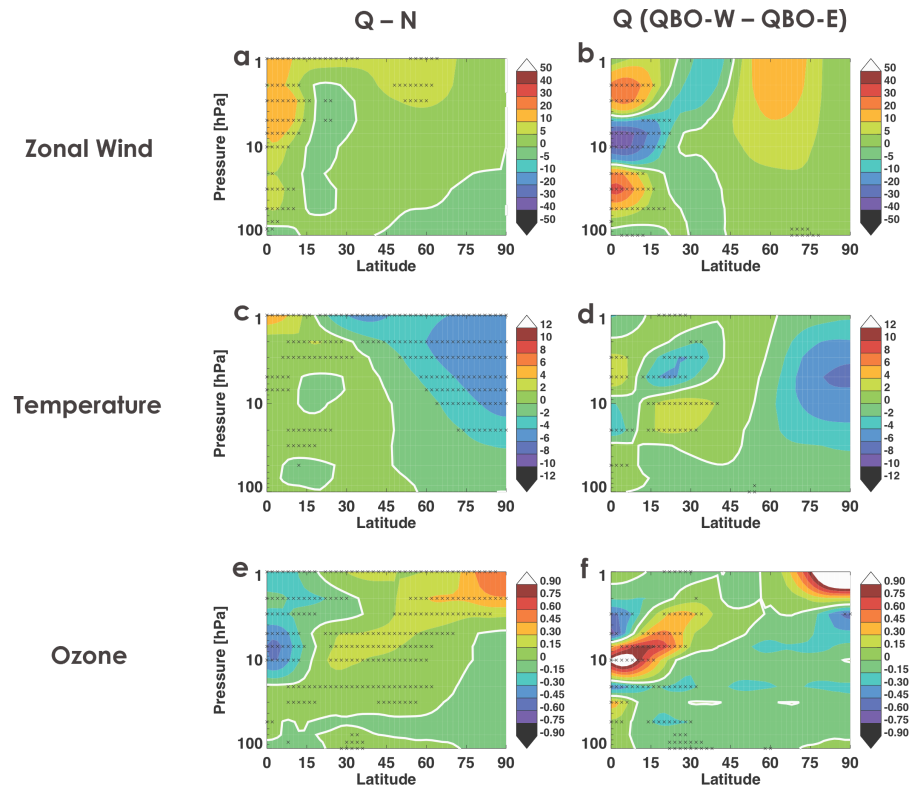


Fig. 8. January (a, b) zonal wind [ms^{-1}], (c, d) temperature [K] and (e, f) ozone [ppmv] differences in the Northern Hemisphere. (a, c, e) Q–N mean differences; (b, d, f) QBO-westerly – QBO-easterly differences in the Q simulation. White contours indicate zero difference. Black Xs indicate differences significant at the 95 % level in a two-tailed t test.

[Title Page](#)
[Abstract](#)
[Introduction](#)
[Conclusions](#)
[References](#)
[Tables](#)
[Figures](#)
[Back](#)
[Close](#)
[Full Screen / Esc](#)
[Printer-friendly Version](#)
[Interactive Discussion](#)